Physical and chemical properties of lunar magma

van Kan, M.

2011

Chapter 4

Density of primitive lunar melts

Mirjam van Kan Parker, Nicolas Sator, Bertrand Guillot, Wim van Westrenen

ABSTRACT

Thermo-chemical models of the dynamics of the internal differentiation of the Moon require accurate knowledge of the density of lunar minerals and melts at a range of high pressure, high temperature conditions. Here we present a comparative study of high-pressure, high-temperature density determinations of possible primitive lunar melts, as represented by volcanic glass beads sampled during the Apollo missions. We performed molecular dynamic (MD) simulations on the density of molten low (Apollo 15C green), intermediate-high (Apollo 17 74,220 orange) and high titanium (Apollo 14 black) bearing lunar glass compositions at conditions bracketing those relevant for lunar interior melt evolution (pressures between 0 and 10 GPa and temperatures of 1723, 2073 and 2423 K).

Density variations are well described by third-order Birch-Murnaghan equations of state. Isothermal bulk moduli at 1673 K, K_{1673}, are 18.2 ± 0.2 GPa for green glass, 20.8 ± 1.0 GPa for orange glass, and 19.6 ± 0.3 GPa for the black glass composition. Corresponding pressure derivatives, K', are 8.5 ± 0.2, 7.6 ± 0.6, and 9.2 ± 0.3, respectively. These values translate to calculated densities of 2.97-3.06 g cm^{-3} (green), 3.10-3.19 g cm^{-3} (orange) and 3.19-3.28 g cm^{-3} (black) at liquidus temperatures and typical multiple saturation depths between 1.5 and 2.5 GPa.

We compare these results with previously published *ex situ* and *in situ* experimental density measurements that were performed on synthetic analogues of these glasses. Within the lunar pressure range the results of these widely different techniques are comparable with MD simulations to within 5.9%. Irrespective of the technique used, the largest uncertainty in lunar melt density prediction at high pressure is the uncertainty in the room-pressure density values used to anchor both MD simulations and experiments, in particular for titanium- and iron-rich compositions.

1. INTRODUCTION

Crystallisation and differentiation of the lunar magma ocean are thought to have resulted in a gravitationally unstable mineral stratification of the lunar mantle (e.g. Snyder et al., 1992; Shearer and Papike, 1999), inducing large-scale mantle overturn (e.g. Hess and Parmentier, 1995; de Vries et al., 2010). This overturn is believed to have triggered and aided the formation and eruption of the high titanium bearing lunar basalts (e.g. Snyder et al., 1992), while partial melting of the early cumulates resulted in the formation of low titanium bearing mare basalts (e.g. Grove and Krawczynski, 2009).

Experimentally determined multiple-saturation points (msp) for the high titanium bearing glasses show deep levels of formation (Wagner and Grove, 1997; Grove and Krawczynski, 2009), e.g. 250 to 500 km. Various researchers (e.g. Circone and Agee, 1996; Wagner and Grove, 1997) suggested that the relatively high density of high-titanium lunar basalts should have made it impossible for them to erupt from their depth of origin without additional external aid. Elkins-Tanton et al. (2002) suggested that the msp for the high titanium bearing glasses did not record their actual depth of formation in contrast to the msp of the low titanium bearing glasses. They postulated that the high titanium bearing glasses formed from mixed source regions at shallow levels, facilitating eruption at the lunar surface.

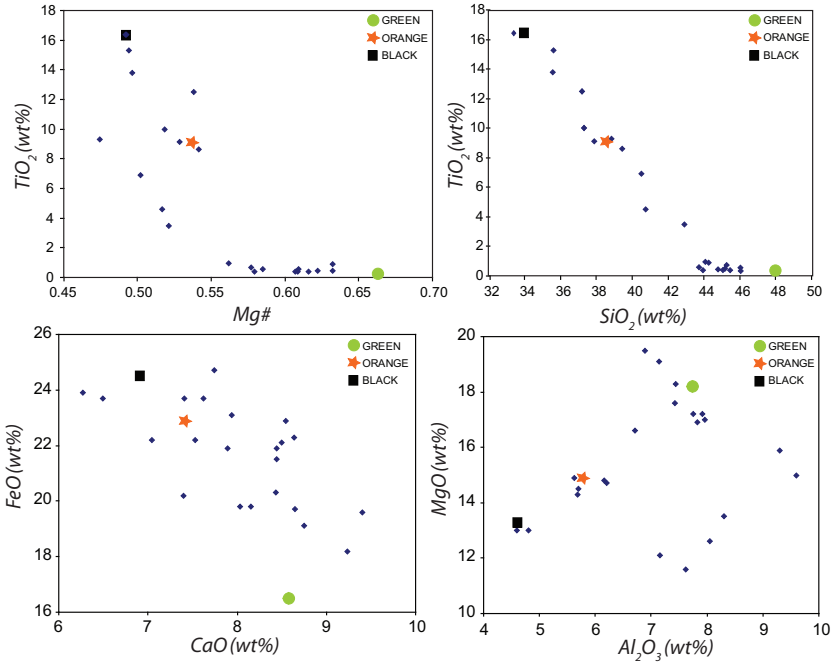

Figure 1. Selected compositional variations of the 25 groups of lunar glasses (small diamond symbols, data from Delano, 1986). The three larger symbols represent the compositions used in our molecular dynamic simulations (filled circle, Apollo 15C green; star, Apollo 17 74,220 orange; and square, Apollo 14 black).

Numerical thermo-chemical simulations of these different petrological models require the availability of accurate estimates of the high-pressure (*P*), high-temperature (*T*) densities of lunar interior primitive melts. Over the past decades, four different methods have been used to quantify the density of molten lunar glasses at high *P-T*: (1) Numerical calculations (Delano 1990), (2) *ex situ* sink/float experiments (Circone and Agee, 1996; Smith and Agee, 1997; Ohtani and Maeda, 2001; van Kan Parker et al., 2011a), (3) *in situ* synchrotron experiments (Sakamaki et al., 2010b; van Kan Parker et al., 2011b) and (4) molecular dynamic simulations (Guillot and Sator, 2007a; 2007b).

Here we present new molecular dynamic (MD) simulation calculations on the density of three molten lunar glasses (Apollo 15C green, Apollo 17 74,220 orange and Apollo 14 black, see Table 1) bracketing the large variation observed in Ti content (Fig. 1) as a function of *P* and *T*. Additionally we provide a detailed synthesis and comparison with earlier *ex situ* and *in situ* measurements. Our aim is to assess the remaining uncertainties in lunar melt density models, and aid future thermo-chemical models of lunar magmatic differentiation.

2. COMPUTATIONAL METHODS

Sample compositions are given in Table 1 and illustrated in Fig. 1. Densities were calculated using classical molecular dynamics (MD). For a full summary of the computational methods see Guillot and Sator (2007a; 2007b). Briefly, MD is based on iteratively solving the equations of motion of an assembly of particles interacting through a given force field. Changes in the positions and velocities of the particles with time enable evaluation of macroscopic properties by performing a time average of the corresponding quantity during the MD run. Following Guillot and Sator (2007a), a simple force field is used to describe the silicate melt structure of the main oxide components; SiO_2, TiO_2, Al_2O_3, FeO, MgO, CaO, Na_2O, and K_2O. For simplicity, the contributions of the minor components Cr_2O_3 and MnO were not included in the MD simulations. The interatomic energy between atoms *i* and *j* (where *i, j* = Si, Ti, Al, Fe, Mg, Ca, Na, K, O) as a function of

Table 1. Average major element compositions of the low, intermediate-high and high titanium bearing glasses (from Delano, 1986). A15G = Apollo 15C green glass, A15GA = Apollo 15A green glass, A17O = Apollo 17 74,220 orange glass and A14B = Apollo 14 black glass.

	SiO_2	TiO_2	Al_2O_3	Cr_2O_3	FeO	MgO	MnO	CaO	Na_2O	K_2O	Mg#
Wt%											
A15G	48.0	0.26	7.74	0.57	16.5	18.2	0.19	8.57	-	-	0.66
A15GA	45.5	0.38	7.75	0.56	19.7	17.2	0.22	8.65	-	-	0.61
A17O	38.5	9.12	5.79	0.69	22.9	14.9	-	7.4	0.38	-	0.54
A14B	34.0	16.4	4.6	0.92	24.5	13.3	0.31	6.9	0.23	0.16	0.49

Note: Cr_2O_3 and MnO were not included in the MD simulations. Na_2O and K_2O concentrations were rounded to the nearest decimal place in the MD simulations.

their distance is given by:

$$v(r_{ij}) = z_i z_j / r_{ij} + B_{ij} e^{-r_{ij}/\rho_{ij}} - C_{ij} / r_{ij}^6 \quad (1)$$

where r_{ij} is the distance between atoms i and j, $z_{i,j}$ are the effective charges associated with atoms i and j, respectively. B_{ij}, ρ_{ij} and C_{ij} are parameters describing repulsive and dispersive forces between the ij pairs.

To ensure the transferability of the interaction potentials between different melt compositions, the valence assigned to the atoms is fixed. Potential parameters were identical to those listed in Guillot and Sator (2007a; 2000b), obtained by constraining MD simulations to reproduce the experimentally determined density and microscopic structure at atmospheric pressure of 11 natural silicates in the liquid phase (Guillot and Sator, 2007a). The applied force field is similar to that employed in the study of Matsui (1994) which only considered the simple system CaO-MgO-Al_2O_3-SiO_2 (see also Guillot and Sator, 2007b). For the simulations we used N ~1000 atoms, tracked over a typical time scale of 1 ns (corresponding to 1 million MD steps). Statistical fluctuations during the runs were ± 0.5 GPa for P, $\Delta T/T = \pm 1\%$ and $\Delta\rho/\rho = \pm 1\%$.

A series of MD simulations in the isothermal–isobaric (NPT) ensemble were performed to assess melt density evolution with P in the range of 0-10 GPa along the 1723, 2073 and 2423 K isotherms. Each composition was first equilibrated at P = 0 GPa at a given T. All data points were independent from one another (Table 2) and have been equilibrated in the NPT ensemble at chosen P-T. Calculations in both the isothermal–isobaric NPT and microcanonical (NVE) ensembles were cross checked to evaluate statistical uncertainties, using production runs of 0.1–1 ns and long simulation runs of 10 ns were performed when evaluating time dependent properties.

Resulting pressure-volume-temperature data were fitted using a third-order Birch–Murnaghan equation of state (BMEOS; Birch, 1947) using the EOSfit software (Angel 2000):

$$P = \frac{3}{2} K_T \left[\left(\frac{\rho_{T,P}}{\rho_{T,0}} \right)^{7/3} - \left(\frac{\rho_{T,P}}{\rho_{T,0}} \right)^{5/3} \right] \left[1 - \frac{3}{4}(4 - K') \left(\left(\frac{\rho_{T,P}}{\rho_{T,0}} \right)^{2/3} - 1 \right) \right] \quad (2)$$

in which P is pressure, K_T the isothermal bulk modulus at temperature T, K' its pressure derivative, and $\rho_{T,0}$ and $\rho_{T,P}$ are the melt densities at temperature T and ambient pressure (10^5 Pa) and high pressure respectively. Densities at high temperature are related to densities at a reference temperature using

$$\rho_{T,0} = \rho_{Tref\,0} \exp \int_{Tref}^{T} \alpha(T) dT \quad (3)$$

in which the thermal expansion α is defined as:

$$\alpha(T) = \alpha_0 + \alpha_1 T \quad (4)$$

Table 2. Computational density values along three isotherms for the green, orange and black glass compositions. Statistical fluctuations are ±0.5 GPa for *P*, ±1% for *T*.

	A15 Green C glass		A17 74,220 Orange glass		A14 Black glass	
T	Density	*P*	Density	*P*	Density	*P*
(K)	(g cm^{-3})	(GPa)	(g cm^{-3})	(GPa)	(g cm^{-3})	(GPa)
1723	2.81	-0.001	2.94	-0.124	3.02	-0.108
	2.94	0.929	3.07	1.005	3.15	0.908
	3.04	2.016	3.17	2.08	3.25	2.051
	3.13	2.914	3.26	3.019	3.33	2.91
2073	2.69	0.012	2.8	-0.05	2.87	-0.011
	2.84	0.992	2.95	0.952	3.02	0.983
	2.95	1.99	3.07	2.07	3.14	2.085
	3.04	3.015	3.16	3	3.28	3.632
	3.19	5.018	3.32	4.968	3.39	4.998
2423	2.58	-0.106	2.67	-0.025	2.73	-0.04
	2.74	0.916	2.84	1.053	2.91	1.01
	2.86	2.025	2.97	2.059	3.03	1.966
	2.96	3.015	3.07	2.941	3.14	2.8
	3.12	5.062	3.24	5.113	3.3	5.007
	3.3	8.179	3.43	7.927	3.49	7.998
	3.4	10.193	3.54	10.131	3.6	10.123

3. RESULTS

As explained by Sakamaki et al. (2009), even though reference temperatures are set to 300 K when describing and EOS for solid materials, it is unrealistic to do so for silicate melts. This is simply because silicate melts densities at 300 K can not be determined. We therefore adopted a $T_{reference}$ of 1673 K for all three glasses. Extrapolating phase diagrams from experimental studies show that at 1 bar, all three studied glasses are fully molten at this *T* (Wagner and Grove, 1997; Elkins-Tanton et al., 2003b; Krawczynski and Grove, 2008). Density data are presented in Table 2 and shown as symbols in Fig. 2. Best-fit values for the BMEOS parameters are summarised in Table 3 and are used to draw the density curves in Fig. 2.

Our computer simulations reveal subtle differences in the density evolution of the three compositions. K_{1673} is smallest for the green glass composition (18.2 ± 0.2 GPa) and largest for the orange glass composition (20.8 ± 1.0 GPa). The bulk modulus for the black glass composition (19.6 ± 0.3 GPa) is close to that of the orange glass. K' values are similar for the three compositions with 7.6 ± 0.6 for orange glass, 8.5 ± 0.2 for green glass and 9.2 ± 0.3 for black glass. These values are consistent with previous MD simulations of Guillot and Sator (2007b) that yield K' values between 7 and 8 for most basic and ultrabasic melts. Values for d*K*/d*T* are identical for orange and black glass (-0.0104 ± 0.0015 and -0.0103 ±

0.0000 GPa K^{-1} respectively), while for green glass the value is significantly lower at -0.0072 ± 0.0003 GPa K^{-1}. The 1 bar densities at 1673 K are 2.83 ± 0.01, 2.96 ± 0.02 and 3.04 ± 0.01 g cm^{-3} for green, orange and black glass respectively.

The small differences in BMEOS parameters result in non-linear variations in the predicted density differences between the compositions. Fig. 2 shows that density differences ($\Delta\rho$) between the green and black glass compositions gradually decrease with increasing P at 1723 K. For the green glass - orange glass difference we see a similar trend

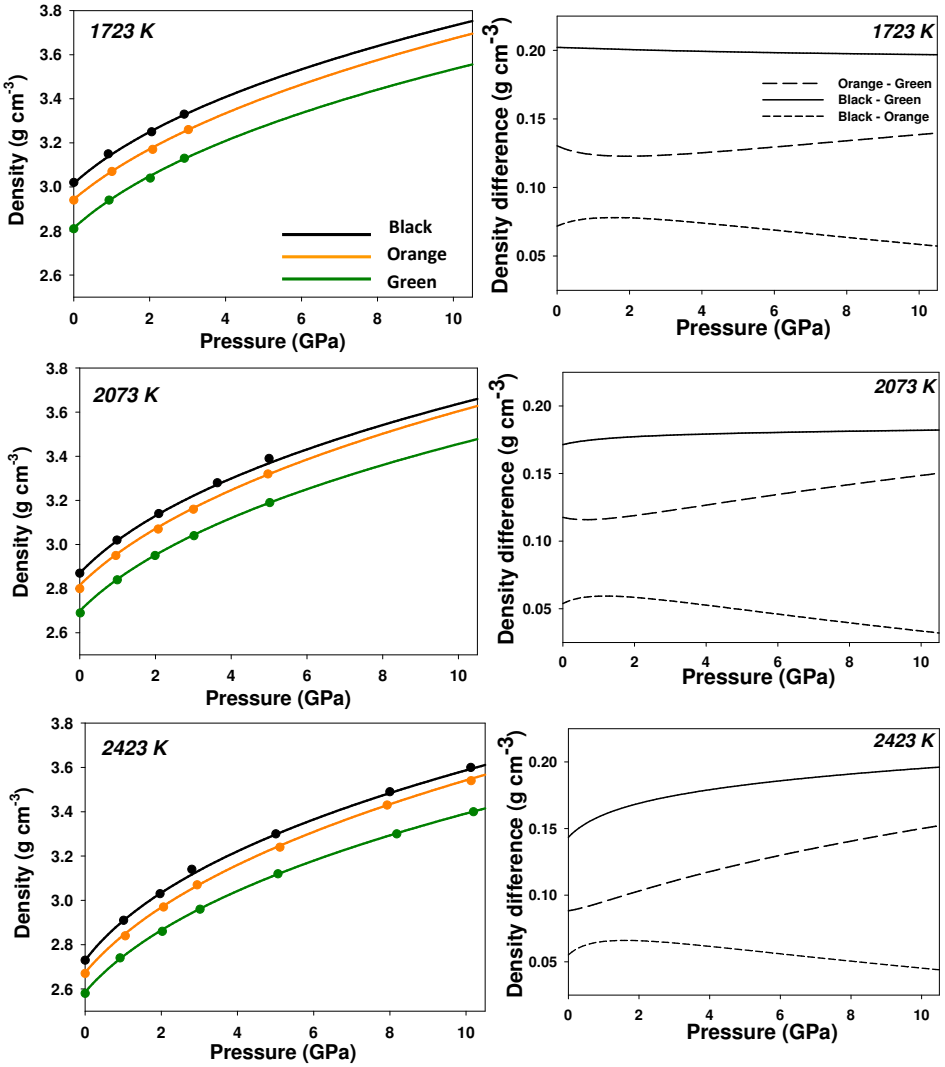

Figure 2. Left: density measurements along three isotherms, 1723 K, 2073 K and 2423 K calculated via MD for the green, orange and black glass compositions (symbols). Curves are drawn using best-fit BMEOS parameters (Table 3). Right: density differences between the glasses as function of pressure.

Table 3. Best-fit values for BMEOS parameters. A15G = Apollo 15C green glass, A17O = Apollo 17 72.440 orange glass and A14B = Apollo 14 black glass. K_T and ρ_0 are at our reference temperature of 1673 K.

	K_{1673} (GPa)	dK/dT GPa/K	K'	a_0 x^{-05}	a_1 x^{-08}	ρ_{1673} g cm^{-3}
A15G	18.2(2)	-0.0072(3)	8.5(2)	10.7(16)	0.63(78)	2.83(1)
A17O	20.8(10)	-0.0104(15)	7.6(6)	1.5(57)	5.9(30)	2.96(2)
A14B	19.6(3)	-0.0103(0)	9.2(3)	12.4(19)	0.88(96)	3.04(1)

Numbers in parentheses indicate one standard deviation (1σ) of replicate analyses in terms of last significant numbers: 26.04(180) should be read as 26.04 ± 1.80.

at low pressure, but at $P > 3.0$ GPa the density difference shows a slight increase. For the green - black glass at 2073 K and 2423 K, and for orange - green glass at 2423 K we find a gradual increase in $\Delta\rho$ with increasing P. The orange glass - black glass $\Delta\rho$ shows similar behaviour at different temperatures, with a slight increase in $\Delta\rho$ up to ~1.5 GPa followed by a $\Delta\rho$ decrease at larger P. Finally the orange – green glass $\Delta\rho$ at 2073 K show a decrease up to 0.7 GPa and then $\Delta\rho$ gradually increases with increasing P. $\Delta\rho$ between the three compositions is largest for the 1723 K isotherm. It is thus clear that density varies non-linearly with composition when considering these three molten lunar glasses.

4. COMPARISON WITH PREVIOUS DENSITY DETERMINATIONS

Extrapolation from room pressure density models

In his classic 1990 paper, Delano (1990) made the first attempt to estimate the densities of molten lunar glass compositions in the lunar interior, using extrapolations from room pressure density measurements. He used compositional parameters derived for individual oxide components by Lange and Carmichael (1987) to evaluate the isothermal bulk modulus for the Apollo primitive glasses, and calculated the densities of molten Apollo 15A green, Apollo 17 orange 74,220 and Apollo 14 black glass compositions at their liquidus T as a function of P. Resulting values for the isothermal bulk modulus at the liquidus were 21.8 GPa (green), 20.9 GPa (orange) and 20.2 GPa (black). Additionally for the Apollo 15C green glass he found K_{liq} = 21.7 GPa. Delano (1990) estimated their pressure derivative, K' to be between 5 and 7, and fixed dK/dT at -0.0025 GPa K^{-1}. Delano (1990) further calculated 1 bar liquidus densities of 2.817, 3.015 and 3.121 g cm^{-3} for the Apollo 15C green, Apollo 17 orange 74,220 and Apollo 14 black respectively. Comparing these 1 bar liquidus densities to the values obtained by using MD we find that green glass values are comparable, whereas orange and black glass values obtained by our MD are 1.5 and 1.8% lower respectively.

Table 4. Comparison of experimental density values derived from neutral buoyancy results of sink/float experiments of green glass (Smith and Agee, 1997), SA-G and (Ohtani and Maeda, 2001), OM-G; orange glass (van Kan Parker et al., 2011a), VKP-O; and black glass (Circone and Agee, 1996), CA-B, with values derived for the same *P-T* conditions using MD.

Source	*P* (GPa); *T* (K)	Reported density (g cm^{-3})	Density MD (g cm^{-3})	Δρ
SA-G	3.0; 1918	3.12(4)	3.082	-1.3(13) %
OM-G	14.5(5); 2773	3.49(1)	3.545	+1.6(3)%
VKP-O	1.0; 1727	3.09(6)	3.069	-0.7(19)%
VKP-O	1.3; 1739	3.09(2)	3.098	+0.3(7)%
VKP-O	7.0; 2223	3.65(6)	3.414	-6.5(15)%
VKP-O	8.0; 2223	3.72(7)	3.471	-6.7(18)%
CA-B	1.5; 1707	3.30(4)	3.208	-2.8(12)%
CA-B	5.5; 2073	3.65(8)	3.406	-6.7(20)%
CA-B	6.0; 2108	3.66(4)	3.429	-6.3(10)%
CA-B	10.0; 2328	3.83(4)	3.599	-6.0(10)%
CA-B	11.5; 2353	3.86(7)	3.664	-5.1(17)%

Numbers in parentheses are 1σ errors on the reported density value, derived from the uncertainties in mineral sphere density calculations and compositional deviation from the ideal green, orange or black glass composition; 3.12(4) should be read as 3.12±0.04.

Ex situ experimental results

Ex situ high-*P*, high-*T* sink/float experiments were previously performed on synthetic analogues of the Apollo 15C green glass (Smith and Agee, 1997; Ohtani and Maeda, 2001), the Apollo 17 74,220 orange glass (van Kan Parker et al., 2011a) and the Apollo 14 black glass (Circone and Agee, 1996). Tight constraints on melt densities were obtained at a limited number of pressure-temperature conditions, summarised in Table 4. We use the best-fit BMEOS parameters derived from the MD simulations (Table 3) to calculate the predicted MD density values for the green, orange and black glass corresponding to these same experimental *P-T* conditions. Sink/float data consistently suggest higher density values compared to the values calculated using MD, with the exception of the highest pressure sink/float density point from Ohtani and Maede (2001). Within the lunar pressure regime ($P < 4.7$ GPa), the sink/float density results (Circone and Agee, 1996; Smith and Agee, 1997; van Kan Parker et al., 2011a) agree fairly well with the calculated values. The methods agree to within 1.3% for the green glass, 0.7% for the orange glass, and 2.8% for the black glass (Table 3).

Density differences between the two techniques can be partially explained by deviations of the experimental run product compositions from the ideal Apollo glass compositions compared to those used in the simulations. In addition, the minor contributions of the relatively dense components Cr_2O_3 and MnO were neglected in the MD simulations. Third, liquid densities derived from sink/float studies are linked directly to densities of the mineral spheres used as markers. These densities are not always well-constrained at the pressures and temperatures of interest. Uncertainties in the EOS

parameters of density markers therefore translate into additional uncertainties in the resulting liquid density values.

The *ex situ* experimental studies of the orange and black glass yielded sufficient data to constrain EOS parameters at selected high temperatures. Circone and Agee (1996) reported 2173 K parameters K_{2173} = 13-23 GPa and K' = 7-3 respectively for the black glass, with best-fit values of K_{2173} = 15.5 GPa and K'= 5.2. For the 1713 K isotherm they reported K_{1713} = 14.9 GPa and K'= 4.7. Our MD results yield K_{2173} = 14.5 GPa and K_{1713} = 19.2 GPa, somewhat lower and higher compare to the experimentally derived values, respectively.

Van Kan Parker et al. (2011b) reported 2173 K parameters K_{2173} = 16.1-20.3 GPa and K' = 3.6-8 for orange glass, with best-fit values of K_{2173} = 18.8 GPa and K'= 4.4, when using the data of Lange and Carmichael (1987) to calculate the 1 bar density value. When using the data of Ghiorso and Kress (2004) to calculate the 1 bar density point, van Kan Parker et al. (2011b) found K_{2173} = 14.4-18.0 GPa and K' = 3.7-8.7, with best-fit values of K_{2173} = 17.2 GPa and K'= 4.5. Our MD results yield K_{2173} = 15.6 GPa, slightly lower than the experimentally derived values. MD values for the pressure derivative of the bulk modulus show significantly higher values of 7.6 ± 0.6 for orange and 9.2 ± 0.3 for the black glass, suggesting a less compressible liquid than suggested by the sink/float experiments.

In situ experimental results

In recent years liquid density measurements at extreme conditions have benefitted from the development of *in situ* synchrotron X-ray absorption techniques (e.g. Katayma et al., 1993; Katayama, 1996; Sanloup et al., 2000b, 2002; Ohtani, 2005; Sakamaki et al., 2009; 2010a; 2010b; and overview in Ohtani, 2009). Recently Sakamaki et al. (2010b) presented the first *in situ*, density measurements on a synthetic equivalent of the black glass composition at superliquidus conditions using synchrotron radiation, obtaining density results between 0.8 and 4.7 GPa, and 1700 and 2100 K. With these results they derived a BMEOS at 1700 K with K = 9.0 ± 1.2 GPa, K' = 16.0 ± 3.4 and dK/dT = -0.0030 ± 0.0008 GPa/K, indicating a significantly more compressible liquid than predicted by our MD or the *ex situ* experiments of Circone and Agee (1996). Van Kan Parker et al. (2011b) also presented *in situ*, density measurements on synthetic equivalents of both the lunar green and black glass at superliquidus conditions using synchrotron radiation. They obtained five density values, two for the green glass at 1.6 GPa, and three at pressures between 1.0 and 1.7 GPa for the black glass. However, the few datapoints did not allow for the formulation of a BMEOS.

The density values obtained with both aforementioned studies are given in Table 5, which also lists computationally predicted density values at the corresponding *P-T* conditions calculated using the BMEOS parameters derived using MD (listed in Table 3). The black glass density values obtained by van Kan Parker et al. (2011b) are within error of the MD results, whereas the results from Sakamaki et al. (2010b) are somewhat higher, with density differences up to 5.9%. The two green glass values (van Kan Parker et al.,

Table 5. Comparison of reported density values derived from synchrotron radiation experiments (in italic: van Kan Parker et al., 2011b; in bold Sakamaki et al., 2010b) green glass and black glass with values derived from MD. Reported errors on MD are derived from the uncertainties of the *P-T* conditions of the *in situ* measurements.

Glass type	P (GPa); T (K)	Reported density ($g\ cm^{-3}$)	Calculated MD density ($g\ cm^{-3}$)	Δρ
Green glass	1.6; 1908	2.87(3)	2.957(46)	-3.3(17)%
Green glass	1.6; 1988	2.84(4)	2.935(45)	-3.7(20)%
Black glass	1.0; 1854	3.15(14)	3.100(56)	+0.4(4.5)%
Black glass	1.6; 1775	3.14(3)	3.189(47)	+1.8(16)%
Black glass	1.7; 1850*	3.11(3)	3.177(80)	+2.4(24)%
Black glass	1.19; 1700	3.33(5)	3.178(17)	4.6(14)%
Black glass	0.83; 1800	3.23(4)	3.099(12)	4.0(12)%
Black glass	2.85; 1800	3.50(7)	3.298(11)	5.8(19)%
Black glass	2.84; 1900	3.46(3)	3.265(15)	5.6(8)%
Black glass	3.18; 1800	3.52(3)	3.324(13)	5.6(8)%
Black glass	3.15; 1900	3.49(2)	3.290(12)	5.7(5)%
Black glass	4.76; 1900	3.60(4)	3.406(8)	5.4(11)%
Black glass	4.50; 2000	3.57(4)	3..360(8)	5.9(11)%
Black glass	4.24; 2100	3.50(2)	3.314(9)	5.3(5)%

Errors on *P* are ±0.3 GPa, errors on *T* are ±50 K except *, which has a T error of ±140 K; Numbers in parentheses indicate estimated 1 sigma density error: 2.87(3) should be read as 2.87 ± 0.03.

2011b) are 3.3 ± 1.7% and 3.7 ± 2.0% lower, for the experiments at 1.6 GPa and 1908 K and 1988 K respectively, compared to our MD results.

Assessing the cause of the density variations between the *in situ* density determinations and the MD predictions is difficult. As shown by van Kan Parker et al. (2011b) minor density differences between the two techniques can partially explained by deviations of the run products from ideal Apollo glass samples. However, since Sakamaki et al. (2010b) did not report the chemical compositions of the run products it is difficult to assess the cause of the density variations between their experiments, those of van Kan Parker et al. (2011b) and our predicted MD density values. Another possible cause for density differences could be related to the fact that Sakamaki et al. (2010b) relied on the 1 bar density values which they calculated using partial molar volumes of Lange (1997) and Lange and Carmichael (1987), which could in fact be an overestimate of the true 1 bar density value. Finally another possible cause for the density difference between the techniques could be the neglected contributions of relatively dense Cr_2O_3 and MnO in the MD simulations.

Implications for lunar magma density modelling

In Fig. 3 compilation is shown of current predictions of the density evolution along the liquidus of the three glass composition as a function of depth in the Moon. Following

Delano (1990), curves were constructed assuming room *P* liquidi of 1673 K (green glass), 1642 K (orange glass) and 1604 K (black glass) to calculate the 1 bar density values. To calculate the density evolution with pressure we used a range of estimated $T_{liquidus}$ values, assuming an increase with pressure between 70 and 100 K GPa^{-1}. Solid curves are calculated using our MD results, and dashed curves are based on the work of Delano (1990). Symbols are derived from *ex situ* sink/float experiments.

Within the relevant lunar *P-T* range, the differences in thermoelastic parameters obtained using the different methods for both orange and black glass compositions result in only minor differences in predicted densities in the lunar interior. Only at $P > 4.7$ GPa, e.g. *P* conditions at the centre of the Moon, larger differences appear (e.g. Table 4).

MD simulations show lower density values for both the orange and black glass compositions compared to the calculated values of Delano (1990), while the green glass composition compares relatively well, within 1.6%, to the MD values. The results of the sink/float experiments are also included in Fig. 3 since these experiments were all carried out at near liquidus conditions. The sink/float results from the green (Smith and Agee, 1997) and black glass (Circone and Agee, 1996) density studies show higher densities compared to predictions from the MD simulations. Since the *in situ* experiments were conducted at temperature values significantly above the liquidus they were not included in Fig. 3.

The primary reason for the density differences between the orange and black glass composition of the Delano (1990) calculations and the MD simulations is related to the 1 bar reference density point. Delano (1990) used the data of Lange and Carmichael (1987) to anchor the 1 bar density point at $T_{liquidus}$. However, the data of Lange and Carmichael (1987) were derived for terrestrial compositions, e.g. low titanium bearing compositions, reflected in the comparison of the 1 bar density point for the low titanium bearing green glass composition. The density evolutions with depth are very similar when comparing Delano (1990) and MD simulations.

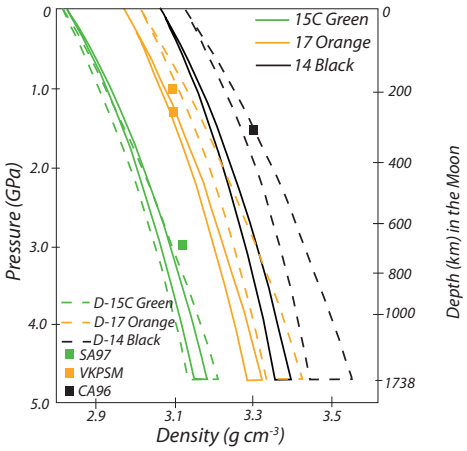

Figure 3. Density evolution of studied lunar glass compositions with pressure at estimated liquidus temperatures. Room pressure liquidus temperatures of 1673 K (green glass composition), 1642 K (orange glass composition) and 1604 K (black glass composition) were taken from Delano (1990). Data are shown for estimated $T_{liquidus}$ increases with pressure between 70 to 100 K GPa^{-1}. Solid lines: MD simulations (this study); dashed lines: calculations of Delano (1990) filled squares: results from sink/float experiments (Smith and Agee, 1997; van Kan Parker et al., 2011a; Circone and Agee, 1996). Note that Delano (1990) originally provided a density curve for the Apollo 15A green glass, here we recalculated the curves for the Apollo 15C green glass composition.

An alternative data set to calculate the 1 bar density point at $T_{liquidus}$ is the one presented by Ghiorso and Kress (2004). For the orange and black glass composition this leads to lowering of the 1 bar density of 0.02 g cm^{-3}, or ~0.7%, at $T_{liquidus}$. The values obtained using the model of Ghiorso and Kress (2004) are thus closer when compared to the 1 bar density values derived with our MD simulations. Both Lange and Carmichael (1987) and Ghiorso and Kress (2004) neglect the minor contributions of Cr_2O_3 and MnO. As illustrated above (see also van Kan Parker et al., 2011a) small variations in the position of the 1 bar density anchor point can lead to significant differences in the predicted variations in density with *P* and *T*, and hence result in larger difference for the isothermal bulk modulus and its pressure derivative, of 8.5 and 2.3% respectively.

Uncertainties in the values of the 1 bar densities of molten lunar magma appear related to uncertainties in the partial molar volumes of TiO_2 and also FeO. These uncertainties can be related to the variable coordination states of Ti and possibly also Fe in silicate melts (Farges et al., 1996; Romano et al., 2000; Liu and Lange, 2001; Guillot and Sator, 2007a; Guo et al., 2009). However, in our MD the coordination state for Ti^{4+} was independent of TiO_2 content of the liquid. At 1723 K the coordination state was 5.7 to 5.9 for 1 bar and 3 GPa respectively, while at 2423 K it was 5.4 (1 bar), 5.8 (5 GPa) and 6.0 (10 GPa). Coordination states of both Ti and Fe are unfortunately currently both unknown for natural picritic lunar magmas. Further reducing the uncertainties depicted in Fig. 3 will require determination of these parameters.

5. CONCLUSIONS

We used MD simulations to derive equation of state parameters for the end-member lunar glasses with very low (Apollo 15C green glass), intermediate-high (Apollo 17 74,220 orange glass) and high titanium (Apollo 14 black glass) contents. Resulting elastic parameters vary with composition, with isothermal bulk modulus $K_{T,}$ ranging from 18.2 ± 0.2 GPa for the green, 20.8 ± 1.0 GPa for orange glass and finally 19.6 ± 0.3 GPa for the black glass composition at 1673 K. Pressure derivatives, *K'* were found to be 8.5 ± 0.2 for green, 7.6 ± 0.6 for orange and finally 9.2 ± 0.3 for the black glass composition.

We compare these results with previously published *ex situ* and *in situ* experimental density measurements that were performed on these compositions over the past decades. Within the lunar pressure range results of these widely different techniques are comparable to within 5.9%. Sink/float studies suggest that lunar glass magmas are more compressible than does MD. Additionally the *in situ* experiments performed by Sakamaki et al. (2010b) also suggest that the high titanium bearing lunar glass magmas are more compressible than does MD. Irrespective of the technique used, the largest uncertainty in lunar melt density prediction at high pressure is the uncertainty in the room pressure density

values used to anchor both simulations and experiments, in particular for titanium- and iron-rich compositions.

ACKNOWLEDGEMENTS This work was supported by a European Science Foundation EURYI award to WvW.